River Sedimentation – Wieprecht et al. (Eds)
© 2017 Taylor & Francis Group, London, ISBN 978-1-138-02945-3

Processes and effects of reversing currents on the erosion stability of wide-graded grain material

A. Schendel
Franzius-Institute for Hydraulic, Estuarine and Coastal Engineering, Leibniz University Hannover, Germany

N. Goseberg
Franzius-Institute for Hydraulic, Estuarine and Coastal Engineering, Leibniz University Hannover, Germany
Department of Civil Engineering, University of Ottawa, Canada

T. Schlurmann
Franzius-Institute for Hydraulic, Estuarine and Coastal Engineering, Leibniz University Hannover, Germany

ABSTRACT: Physical model tests were carried out in a closed-circuit flume to investigate the overall erosion stability of wide-graded bed material in estuarine and coastal conditions by means of simulating tidal flow conditions with reversing currents. As a result of the reversing flow conditions, previously protected sediment eventually becomes exposed again, leading to bidirectional displacement processes in dependency of the flow direction. Furthermore, sediment fractions are slightly coarser under the following reversed flow than under the initial flow. This indicates higher critical shear stresses and thus erosion stability for the initial flow direction. In comparison to unidirectional current, this study finds a higher erosion stability for sediment fractions smaller than the median d_{50} diameter of the initial bed material under reversed current conditions.

1 INTRODUCTION

Scour protection of hydraulic structures in fluvial, estuarine and coastal waters is an essential component assuring a reliable and durable design. The production of wide-graded grain mixtures, which are mainly composed of quarry-stone materials, is flexible and cost-efficient; thus it appears to be an economically and hydraulically first-choice option for numerous concepts for bed protection constructions as well as toe and slope stabilizations in hydraulic and ocean engineering. In addition to the filter stability, the assessment of erosion stability of wide-graded materials against external hydrodynamic loading is of major importance, in particular if applied as discrete single-layer filter.

Existing design approaches for scour protection employ the definition of grain sizes that can withstand the impacting hydrodynamic forces (De Vos et al., 2011). The selection of the required stone size is still usually based on the threshold of motion criteria by applying the classical Shields (1936) approach. Because this approach only considers uniform materials with spherical shapes, it neglects some characteristic properties of wide-graded material such as special grain size distribution and interrelated self-stabilizing effects under current load. These processes include the hiding effect, which describes the shielding of finer fractions by coarser grains and the exposure effect, which depicts the erosion of larger fractions due to an exposed and instable placement in the bed (Shvidchenko et al., 2001). Furthermore, the selective erosion of finer fractions leads to the coarsening of the bed surface and the development of an armor layer as described in Aberle and Nikora (2006) or Mao et al. (2011). Therefore, numerous studies were performed to extend Shields approach regarding the fractional incipient motion for non-uniform sediments by defining hiding functions that describe how incipient motion for grain sizes in mixtures deviates from those of uniform beds (e.g. Kuhnle, 1993; Parker et al., 1982; Wilcock, 1993). Since these studies were focused on fluvial erosion and sedimentation processes, the established approaches are limited to three decisive criteria in dimension of sediment properties and flow environment, i.e. round edges and fairly even grain size distribution, and constant (or nearly constant), unidirectional flow velocity. On the contrary, only few studies are available that focus on the processes of armor layer development and erosion stability of wide-graded sediments under unsteady flow conditions.

Hassan et al. (2006) carried out laboratory experiments on the influence of hydrological conditions on the armor layer development in gravel bed rivers. They investigated different shapes of hydrographs including a constant discharge and a symmetrically as well as asymmetrically increasing and falling discharge.

While a vertical sorting could be observed for a symmetrical hydrograph, asymmetrically shaped hydrographs did not result in a vertical sorting of the bed surface. Furthermore, the symmetrical hydrographs lead to a coarsening of the transported bed load with increasing discharge.

Guney et al. (2013) investigated the effect of flood waves on bed coarsening and transport rates by means of triangular shaped hydrographs. Four preceding flow phases with different but over the time constant discharge were used to ascertain preload in order to sufficiently coarsen the bed surface and determine reference shear stress of individual fractions of the sediment, which consisted of a bimodal sand and gravel mixture. Subsequently, the same hydrograph was generated for tests with undisturbed bed surface and for tests with a coarser bed due to the preceding flows. Guney et al. (2013) showed that the transport rates in the following unsteady flow tests are strongly influenced by the coarsening of the bed during the preceding flows. Furthermore, the amount of transported material during the descending part of the hydrograph was higher than during the rising part. In addition, a strong dependency between the armor ratio and the dimensionless total bed load was found.

Spiller et al. (2015a) performed experiments on the influence of unsteady flow on form-induced shear stress and dynamic lift (Spiller et al., 2015b) over a rough bed. In order to guarantee identical test conditions an artificial streambed was utilized. They found the magnitude of the form-induced shear stress to be dependent on the discharge for non-uniform flow, which contradicts results from Aberle et al. (2008) for uniform flow. Unsteady flow conditions might also trigger strong dynamic lift forces on rough beds, which could result in a break up of already armored bed surfaces.

2 MOTIVATION

To the authors‘ knowledge there are no studies that fundamentally investigate the influence of reversing or oscillating currents on the armor layer development and stabilizing processes of well-graded grain materials. In addition, the sediment properties themselves have a significant effect on the incipient motion and armor layer development. While Göğüş and Define (2005) highlighted the importance of size and form of individual grains, Chin et al. (1994) showed that the tendency to form an armor layer is increasing along with increasing non-uniformity of the sediment grading. The stability of wide-graded grain mixtures composed of quarry-stone material is therefore likely to significantly differ from typical fluvial sediments.

Large scale hydraulic model tests were thus carried out to firstly investigate erosive potentials and the bed stability of wide-graded quarry-stone material subjected to unidirectional currents. First results demonstrate the potential of the material as scour and bed protection (Schendel et al., 2015). As a follow up investigation, the present paper focuses on the underlying processes and the overall erosion stability of wide-graded material in estuarine and coastal conditions by means of simulating tidal flow conditions with reversing currents.

3 EXPERIMENTAL SETUP

The hydraulic model tests were carried out in a closed-circuit flume. Detailed information and technical drawings of this unique flume can be found in Goseberg et al. (2013) who developed a novel laboratory method to generate tsunami-like long waves. The flume is driven by four pipe pumps with a maximum flow capacity of 0.5 m^3/s. Furthermore, the pump control enables continuous adjustment of the flow velocity in both flow directions. In order to allow a comparison, the experimental setup was constructed similar to the tests with unidirectional flow (Schendel et al., 2015).

The model tests were performed in a scale of 1:1 to avoid scaling effects that could bias the behavior of finer sediment fractions in particular in the tested sediment mixture. The tested sediment was a wide-graded quarry-stone mixture made of granodiorite with a grain size distribution in the range of 0.063–200 mm and a geometric standard deviation of σ_g = 7.6. The material was installed in a deep pit with a width of 1.0 m, a length of 2.7 m, and a depth of 0.6 m. The material was built in at the level of the flume bed in a thickness of 200 mm without additional compaction. To ensure a good interlocking with the subsurface, an additional material layer was placed under the material bed, consisting of the same wide-graded material but from a different sample. The test conditions including more sediment grain parameters are given in Table 1. Groyne-like structures and flow straightener were installed to mitigate the inevitable influence of the flume curve on the flow. The water depth H was kept constant at 40 cm (flume width/$H = 2.5$) above the sediment bed throughout the tests. The experimental setup is illustrated in Fig. 1. The eroded bed load was collected by a sediment trap, which was placed 6.0 m downstream of the sediment bed. Apart from obtaining the amount of eroded material, the grain size distribution of the eroded bed load was determined for each test run. Suspended material could not be measured by the sediment trap. To determine the development of the bed topography and identify erosion and deposition areas, digital elevation models (DEM) of the bed topography were measured

Table 1. Test conditions. T is the duration of a single load case, H is the water depth above the material bed and u_{mean} is the mean flow velocity averaged over the cross-sectional area.

d_{10} [mm]	d_{50} [mm]	d_{84} [mm]	σ_g [−]	u_{mean} [cm/s]	T [min]	H [cm]
0.7	25.7	97.8	7.6	10–78	180	40

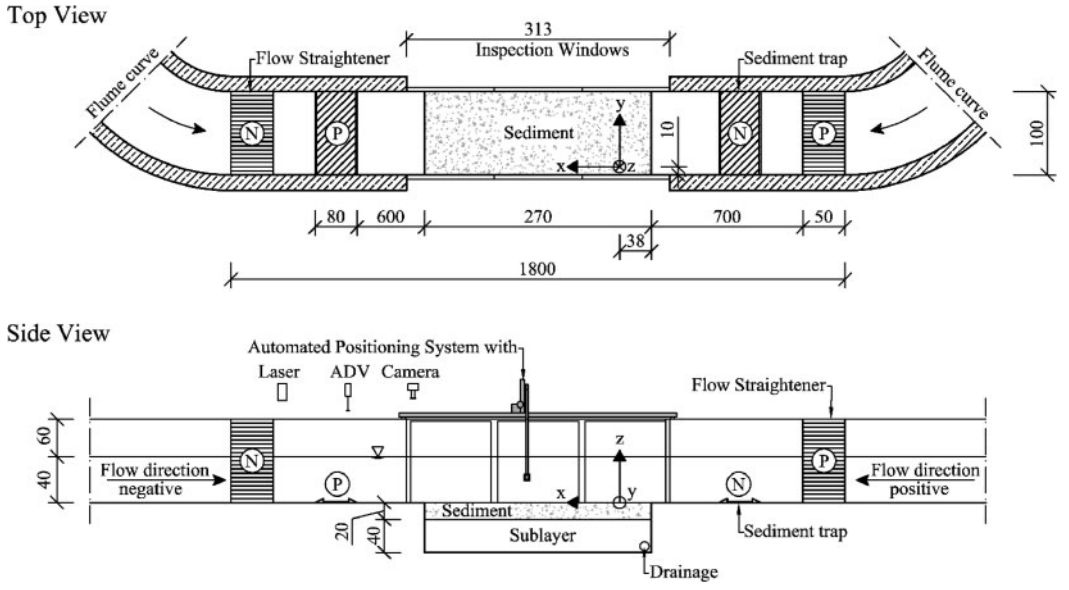

Figure 1. Schematics of experimental setup in top and side views with numbers in centimeter (not to scale). For positive flow direction the sediment trap and the flow straightener were installed at the locations marked with "P", for negative flow direction they were relocated to positions marked with "N".

by means of a high-precision laser distance sensor (OADR 2016480, Baumer). A vertical accuracy of approximately 1.0 mm was achieved by calibration in preliminary tests and subsequent error correction of the laser signal during the analysis.

In order to estimate bed-shear stresses, profiles of three-dimensional (3D) flow velocities were measured by an acoustic Doppler velocimeter (ADV) (Vetrino+, Nortek, max. velocity range ±4 m/s, accuracy ±1 mm/s). A sampling rate of 200 Hz and a measuring period of 30 s for each position were determined to balance between the amounts of recorded samples and the repeatability of experiments. To position the laser distance sensor and the ADV probe automatically and ascertain reproducibly of data logging locations, a three-way traverse system was installed above the sediment bed (Fig. 1). By using this system, the bed topography could be scanned in a grid-like pattern in a very repeatable manner.

3.1 *Test procedure*

The experiment consisted of seven test cases, with successively increasing mean flow velocities u_{mean} ranging from 10 cm/s to 78 cm/s, which were determined during preliminary tests without the sediment bed. The mean flow velocities represent the streamwise velocity averaged over the water depth and the flume width. In order to simulate tidal currents, the flow direction was reversed after each test case before exposing the sediment bed with the next accelerated velocity. The investigated flow velocities are relatively but not unrealistically smaller compared to field measurements, e.g. measurements in the Jade estuary show tidal mean flow velocities of up to 1.3 m/s, and are summarized in Table 2 for negative (initial) and positive flow direction. Despite the small differences of the mean flow velocity, the preliminary tests confirmed comparable velocity distributions in both flow directions. Furthermore, a slight non-uniformity of the streamwise flow velocity between the outer and inner flume wall is evident but was found to be negligible by Goseberg et al. (2013) and Schendel at al. (2015).

Table 2. Mean approach flow velocities for each test case for both flow directions. Negative is the initial flow direction, positive the following reversed one.

	u_{mean} [cm/s]	
Test case	Negative flow direction	Positive flow direction
Test case 1	10	11
Test case 2	15	16
Test case 3	22	24
Test case 4	34	35
Test case 5	56	56
Test case 6	71	73
Test case 7	77	78

At the beginning of the experiment the water was slowly filled into the flume from both sides of the sediment bed to prevent unwanted washout of the finer fractions. No additional sediment was added to the flume upstream of the test bed during the experiment. The duration of each test case and flow direction was at least 3 h, so that a cumulated exposure time of 42 h

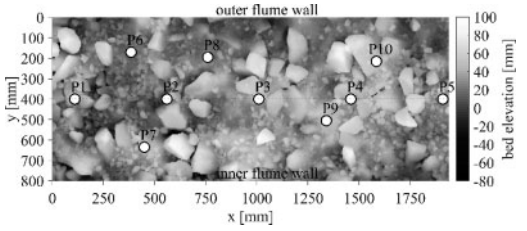

Figure 2. Digital elevation model of initial bed surface. Positions of ADV measurements are marked with circles.

was obtained. After each test case the water was carefully drained to allow an undisturbed measurement of the bed surface by the laser scanner and to extract the eroded material from the sediment trap. Due to the change of flow direction in the following test, the sediment trap and the flow straightener were relocated to the corresponding other side the sediment bed (see Fig. 1). The velocity measurements were performed at the end of each test case after a stabile bed was developed and sediment transport could no longer be observed. The flow velocities were measured at 10 positions over the sediment bed; at five positions along the longitudinal axis of the flume and at five additional positions, which were chosen in dependency of characteristically formed bed formations, i.e. in specific hiding and exposure areas (see Fig. 2). In each of these positions a velocity profile was measured and resolved by eight points over half the water depth. Subsequent to each test case, the bed topography was scanned in longitudinal profiles with a sampling interval of $\Delta x = 0.5$ mm and a lateral spacing of $\Delta y = 5$ mm. Along with a reference scan at the beginning of the experiment a total of 15 laser scans resulting in digital elevation models (DEM) of the bed surface were collected. The scan area covered 60% (194×80 cm, starting from the origin of the coordinate system in Fig. 1) of the total surface of the sediment bed, to exclude systematic wall and boundary effects at the edge of the sediment bed. The sediment trap was emptied after each load case and the grain size distribution was obtained.

3.2 *Method*

To generate detailed DEMs of the bed surface the laser measurements were interpolated to a 1×1 mm grid by means of a cubic Delaunay triangulation. By calculating the elevation differences between the DEMs, erosion and accumulation areas within the bed surface became apparent and a volumetric determination of displacement processes were calculated. To account for measuring inaccuracies in terms of additional settlement or unavoidable signal noise of the laser sensor, only elevation differences greater than ± 2 mm were considered. Fig. 2 shows the DEM of the reference scan in the beginning of the experiment and demonstrates the rough structure of the bed surface.

Because of the strongly inhomogeneous bed surface the assumption of an evenly distributed bed-shear

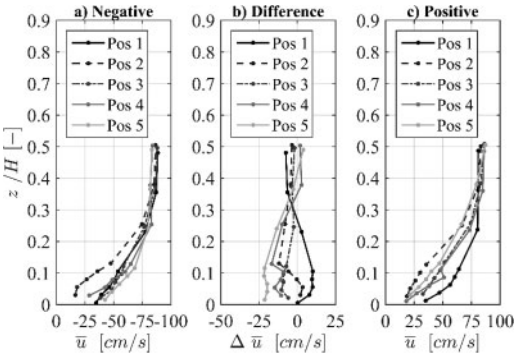

Figure 3. Streamwise, time-averaged velocities for selected measurement positions for test case 6 for both flow directions. b) is showing the differences between both flow directions.

stress would depict an inaccurate mean for the assessment of an initial motion threshold and erosion stability. In an attempt to quantify the inhomogeneity of the given surface, individual bed-shear stresses were determined based on the ADV measurements. The bed-shear stresses were estimated under the assumption of a logarithmic velocity distribution within the boundary layer (as in e.g. Biron et al., 2004). By measuring velocity profiles and fitting a logarithmic equation in the form of $\ln z$ to the data (with z as the height above the bed), local roughness lengths and subsequently shear stresses for each position were determined. The fitting is performed by using a least-square error approach.

The log law method was given the preference over turbulence-based methods, even though it would have been possible to obtain turbulence data from the 3D velocity measurements. This is partially due to the limited resolution of the measured velocity profile and because a reasonable and consistent distribution of Reynolds or TKE stresses over the water depth could not be achieved in the cases reported herein.

Fig. 3 exemplarily compares the measured velocity profiles for test case 6 for the measurement positions P1-P5 on the longitudinal axis of the flume. Despite similar mean flow velocities, $u_{mean} = 71$ cm/s for negative and $u_{mean} = 73$ cm/s for positive flow direction, the reversed flow direction in combination with an altered fluid-sediment interaction led to different near bed flow velocity and thus bed-shear stresses at the same position. Fig. 4 shows the distribution of mean bed-shear stresses τ_{mean}, which are the averaged shear stresses over all positions for a specific test case, and the standard deviations for all test cases. The bed-shear stresses between both flow directions are quite similar for an individual test case, despite the altered fluid-sediment interaction as a result of the reversed flow direction. On the other hand, bed-shear stress variations caused by the inhomogeneous bed are obvious and underline the need for multiple measurement positions to get a sufficient representation of existing bed-shear stresses. More detailed information about

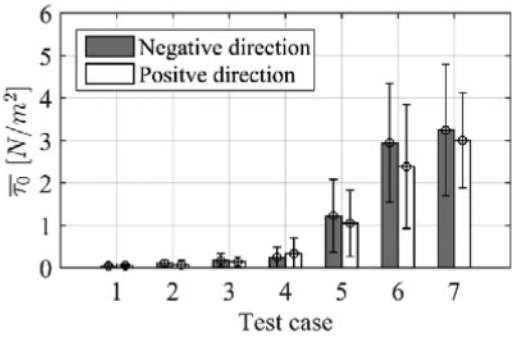

Figure 4. Mean bed-shear stresses $\overline{\tau_0}$ and standard deviation of calculated bed-shear stresses in reference to the test case.

the experimental setup and applied analysis methods can be found in Schendel et al. (2015).

4 RESULTS

4.1 *Development of displacement processes and bed load properties under reversed current*

During the experiment a coarsening of the bed surface with increasing flow velocities has been observed by visual inspection, which is caused by the selective erosion of large quantities of the finer fractions at the beginning of each test case. By the end of each test case sediment transport could no longer be observed. With the formation of a stable and immobile bed surface as indicators, the development of a temporally static armor layer at the end of each test case can be concluded (Jain, 1990; Parker and Sutherland, 1990). Based on the DEMs, Fig. 5 illustrates the cumulated distribution of erosion and accumulation areas in the bed surface at the end of the overall experiment after seven test cases with reversing flow direction. The erosion of sediment occurred more spatially distributed, reflecting areas with a high ratio of finer fractions on the surface. The phenomenon of accumulation was only locally concentrated in sheltered location, i.e. behind larger stones. However, as the result of an altered interaction between flow and bed, causing different near-bed velocities (Fig. 3), and the reallocation of sheltered and exposed areas, previously protected grain fractions (hiding effect) became exposed subsequently and were re-suspended despite being exposed to the same approach flow velocity as in the test case before. Therefore, areas of erosion and accumulation altered repeatedly between the test cases in dependency of the flow direction.

In order to demonstrate these displacement processes, Figs. 6 & 7 show the erosion and accumulation areas for test case 6 in comparison to the respective previous test case 5. The location marked with a black cycle exemplarily illustrates the deposition of sediment behind a larger stone under negative flow direction (Fig. 6). At the end of the following test (Fig. 7) this sediment was eroded again. This periodical

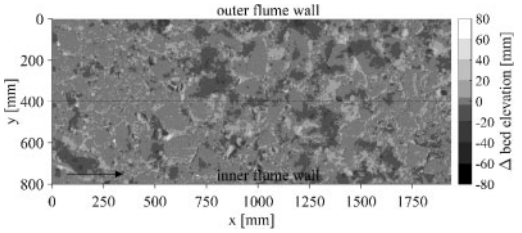

Figure 5. Upper panel: Cumulated erosion (dark gray) and accumulation (light gray) areas at the end of the experiment.

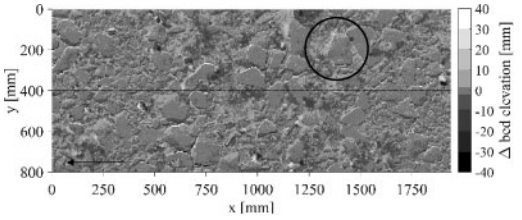

Figure 6. Displacement processes between test case 5 (positive flow direction) and test case 6 (negative flow direction). Dark gray areas represent erosion, light gray areas accumulation.

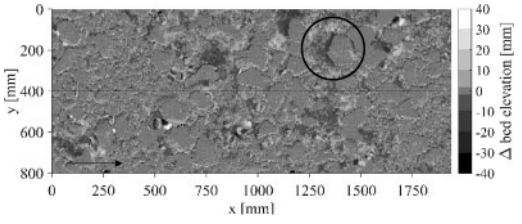

Figure 7. Displacement processes between test case 6 (neagtive flow direction) and test case 6 (positive flow direction). Dark gray areas represent erosion, light gray areas accumulation.

alternation of erosion and accumulation areas on the bed surface could be observed with every change of flow direction throughout the entire experiment. If only one flow direction had been considered the erosion as well as accumulation areas would have remained in the same place, also the depth changes would have intensified with successively increasing flow velocities, especially for the last four test cases.

Fig. 8 compares the amount of displaced sediment within the scanned area for each test to further quantify the net sediment budgets between both flow directions. During the experiment the amount of accumulated material is quite similar between both flow directions within a test case. Furthermore, for the first three test cases the magnitude of accumulated sediment stays almost constant despite increasing flow velocity. Test case 2 depicts a clear exception, by showing significantly more accumulated sediment under negative flow direction than under following positive flow direction. However, the influence of the flow direction on the magnitude of accumulated sediment seems

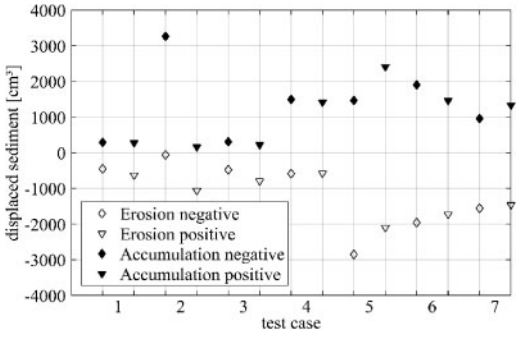

Figure 8. Development of sediment displacement based on the DEMs with individual test cases and flow direction.

too uncorrelated to follow any prevalent driving forces or dependency. The previously protected sediment that became exposed and subsequently entrained due to the reversed flow direction seems to ensure that sufficient fine sediment is available to be eroded and accumulated, respectively. Overall, the same conclusion could be drawn for the total of eroded sediment, although test case 2 and 3 show a slight dependency on the flow direction.

The amount of transported sediment increases significantly with test case 4 in case of accumulation and with test case 5 in case of erosion. Subsequently, the amount of transported sediment is continuously decreasing again with every new test case as well as flow direction. This is interesting, since the shear stresses are driven by increased flow velocity from $u_{mean} = 56$ cm/s to 78 cm/s between test case 5 and 7. Cumulated over all test cases, the amount of eroded and accumulated sediment is almost identical, which may imply that almost no sediment was transported out of the monitored area of the sediment bed or to the adjacent compartments inside the recirculating flume. Instead, as a result of the inhomogeneous and rough bed in combination with the reversing flow direction, a sediment displacement only within the extent of the sediment bed may be assumed. However, as mentioned before, a coarsening of the sediment bed has been evidently observed, which at least suggests the erosion of fine sediment fractions out of the sediment bed.

This is also in agreement with the small amounts of bed load material yielded in the sediment trap, independently of the respected test case. Because of the small amount of eroded material (<30 g) and the large proportion of grain sizes smaller than 0.063 mm in the first three test cases, the sieving of the bed load in conformity to engineering standards could be achieved for test cases 4–6 only. Fig. 9 shows the development of the grain size distributions of the eroded bed load for these test cases in comparison to the initial distribution of the material. While the coarsening of the eroded bed load with increasing velocity is clearly observed, which indicates a continuously coarsening of the bed surface as well, only finer fraction of the initial grain size distribution were eroded. For all test cases only grain sizes smaller than the median d_{50} grain size of

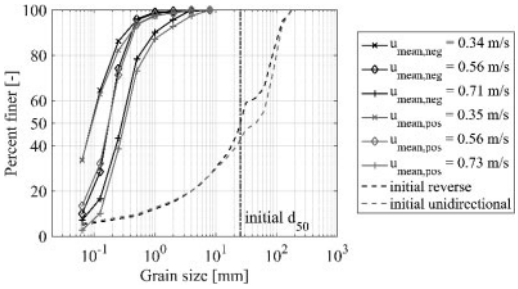

Figure 9. Grain size distributions of eroded bed load collected by sediment traps for three of the seven test cases.

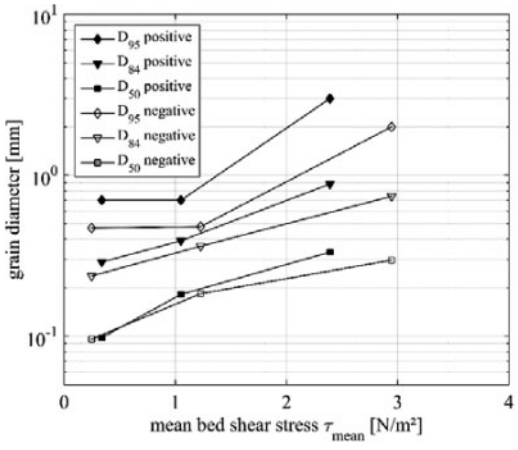

Figure 10. Development of grain size for individual fractions of collected bed load in reference to calculated mean bed shear stresses.

the initial bed were mobilized and eroded. In addition, the influence of the reversing current on the grain size distribution of the eroded bed load material seems only marginal as expected as there is no significant increase in the coarsening of the bed load between the initial flow direction (negative) and the reverse direction (position).

However, the dependency of the grain size distribution on the reverse flow becomes more pronounced once individual grain size fraction are related to the measured bed shear stresses as shown in Fig. 10. Within an individual bed load fraction, a coarsening of grain sizes with increasing load is evident. Furthermore, the variation of grain size with bed shear stress seems consistent for the $d_{50}$and d_{84} fraction of the bed load, while the grain size of the d_{95} fraction remains almost constant for lower bed shear stresses. It is noted, that the grain sizes could only be measure for three different bed shear stresses and that the results therefore might not well represent the behavior for different loads. For the considered sediment fractions, the bed load is slightly coarser in positive (reverse) than in negative direction (initial), despite comparable approach velocities. Furthermore, differences in

grain size between both flow directions are more pronounced for coarser fractions than for finer fractions. Due to the small amount of bed load collected by the sediment trap as well as the bidirectional displacement processes shown by the DEMs, the determination of effective critical shear stresses for the individual fractions might be subjected to uncertainties, i.e. regarding the definition of bed load transport rates and largest transported grain size. It cannot be ruled out that grains larger than that captured by the sediment trap got interlocked within the rough bed surface. Therefore, only a qualitative assessment of critical shear stresses is given. Based on the largest grain size collected by the sediment trap (method applied by Andrews (1983) and Carling (1983)) critical shear stresses were calculated as being larger (up to 5 times) than would have been predicted by the Shields (1936) approach. Here, as it can be concluded from Table 1 and Fig. 10, only grain sizes smaller than the median d_{50} grain size of the initial sediment were eroded.

As a result of coarser grain sizes, critical shear stresses were smaller for the reversed (positive) flow direction than for the initial (negative) flow direction. In brief, as a result of reversing flow conditions, previously protected sediment becomes exposed again, leading to bidirectional displacement processes due to resuspension and a comparable amount of displaced sediment on the bed surface independently of the flow direction (Fig. 8). With regard to the eroded bed load, the sediment fractions are slightly coarser under the succeeding reversed flow than under the initial flow (Figs. 9–10), indicating higher critical shear stresses and thus a higher erosion stability for the initial (negative) flow direction.

4.2 *Comparison to unidirectional current*

In order to compare these bidirectional displacement processes and stability indicators stemming from reversed currents to results of a preliminary study with unidirectional currents, an extended examination is provided in the following. The test under unidirectional current consisted of three experiments utilizing three independent samples of the same wide-graded material resulting in slightly different grain size distribution. Each experiment involved seven test cases, with successively increasing mean flow velocities. The mean velocities in this present study were based on those for unidirectional current, implying comparable approach velocities for each test case between both experiments (cp. Schendel et al. (2015).

Fig. 11 contrasts the grain size distributions of eroded bed load between the bi- and unidirectional tests. To improve comparability averaged grain size distributions are shown. For the reverse current test the grain size distributions of eroded bed load were averaged between both flow directions. In case of unidirectional current tests the grain size distributions were averaged between for the three experiments. In each test case the grain size distribution of eroded bed load is much coarser under unidirectional current than

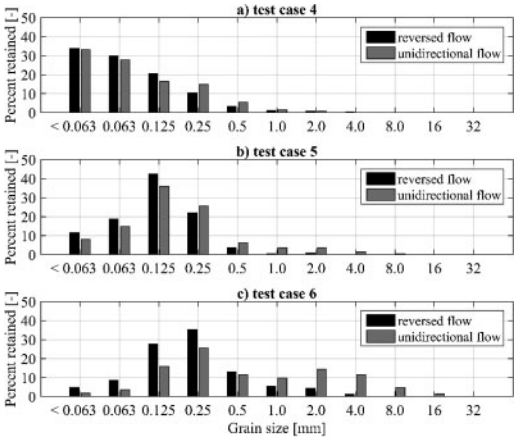

Figure 11. Mean grain size distributions of eroded bed load collected for unidirectional current and reverse current tests.

under reverse current. The differences between the grain size distributions are increasing with higher flow velocity. The erosion of coarser grains under unidirectional current at the same approach velocity implies a smaller erosion stability of these fractions compared to reversing flow conditions.

In contrast to the results for the reversed flow tests, the amount of eroded sediment calculated by means of DEMs clearly exceeds the amount of accumulated sediment, and therefore indicating an overall erosion out of the sediment bed. This is also in agreement with the amount of sediment collected by the sediment trap, which resembles a steady increase of bed load with higher flow velocities and overall significant higher amounts of eroded material than in the reversed current tests. Furthermore, erosion as well as accumulation areas and depth continuously intensify with successively increasing flow velocities. Bidirectional displacement processes as observed under reversed flow are not taking place under unidirectional current.

The results may seem unexpected as one might assume that the variable flow conditions lead to a reduction of the potential to form a statically stable armor layer and thereby decrease the stability against shear failure. One explanation might be that the bidirectional flow causes the mobilized sediment to evenly distribute over the bed surface as it is indicated by the altering displacement processes shown in the DEMs (Fig. 6 & 7). As a consequence, interlocking of grains is increased and larger fractions are not as exposed as before resulting in the formation of a compact and dense surface structure and a high erosion stability.

5 DISCUSSION

Whilst an approximation of tidal currents by means of bidirectional reversing currents does not take the complex and unsteady flow under estuarine and coastal conditions into account, a first study evaluating this

special load case on wide-graded quarry-stone material is conducted with the objective to focus on the selective influence of periodically reversing currents on sediment movement and erosive potentials.

The bed load under unidirectional flow was significantly coarser compared to the results of the reversed current tests. As demonstrated by Fig. 9, the grain size distribution of the initial sediment was also slightly coarser for the unidirectional tests, which might affect the distribution of transported sediment. On the other hand, the grain size distribution is only coarser at grain fractions above those which were mobilized and subsequently transported.

The three experiments under unidirectional flow have shown some significant differences in the amount of eroded material. As pointed out in Schendel et al. (2015) the results might by influenced by the inhomogeneous material properties and uneven structure of the bed surface, which might apply in the same way to the present study. This also includes spatially variable bed shear stresses. In addition, the distribution of the eroded bed load material could only be analyzed for three test cases and the results might not well represent the necessary size for meaningful statistical assessment. Therefore, further investigations have to be carried out to guarantee the reproducibility and verify the results by adding additional data points.

6 SUMMARY AND CONCLUSIONS

Physical model tests were carried out in a closed-circuit flume in order to investigate the influence of wide-graded material effects on erosion stability and displacement processes under estuarine and coastal flow conditions. First insights on the effects of tidal currents by means of periodically reversing flow and stepwise increasing flow velocities were given.

As a result of reversing flow conditions, previously shielded sediment becomes exposed again, leading to bidirectional displacement processes in dependency of the flow direction. Furthermore, sediment fractions are slightly coarser under the succeeding reversed flow than under the initial flow indicating higher critical shear stresses and thus erosion stability for the initial flow direction.

In comparison to unidirectional current, the erosion of coarser grains at the same approach velocities implies a smaller erosion stability for the eroded sediment fractions than under reversing flow conditions. In addition, in contrast to the bidirectional displacement processes under reversed current, erosion as well as accumulation areas and depth continuously intensify with successively increasing flow velocities.

In conclusion, the results of this study indicate an even higher erosion stability of the investigated wide-graded material under reversed current than under unidirectional current, at least for finer grain fractions smaller than the median d_{50} diameter of the initial bed. Although further tests have to be performed to ensure the repeatability of the results, especially regarding the inhomogeneous material properties and bed structure, this study demonstrates once more the potential of the wide-graded material as bed and scour protection for applications under estuarine and coastal conditions.

ACKNOWLEDGMENTS

The authors are thankful to Mibau Holding GmbH for supporting this research and Matthias Hortolani for his support in conducting the extensive hydraulic experiments.

REFERENCES

Aberle, J., and Nikora, V. 2006. Statistical properties of armored gravel bed surfaces. *Water Resources Research* 42.

Aberle, J., Koll, K. and Dittrich, A. 2008. Form induced stresses over rough gravel-beds. *Acta Geophysica* 56(3): 584–600.

Andrews, E. D. 1983. Entrainment of gravel from naturally sorted riverbed material. *Geological Society of America Bulletin* 94(10): 1225–1231.

Biron, P. M., Colleen, R., Lapointe, M. F., and Gaskin, S. J. 2004. Comparing different methods of bed shear stress estimates in simple and complex flow fields. *Earth Surf. Process. Landforms* 29(11): 1403–1415.

Carling, P. A. 1983. Threshold of coarse sediment transport in broad and narrow natural streams. *Earth Surf. Process. Landforms* 8(1): 1–18.

Chin, C. O., Melville, B.W., and Raudkivi, A. J. 1994. Streambed Armoring. *Journal of Hydraulic Engineering* 120(8): 899–918.

De Vos, L., De Rouck, J., Troch, P., and Frigaard, P. 2011. Empirical design of scour protection around monopile foundations Part 1: Static approach. *Coastal Engineering* 58(6): 540–553.

Goseberg, N., Wurpts, A., and Schlurmann, T. 2013. Laboratory-scale generation of tsunami and long waves. *Coastal Engineering* 79: 57–74.

Guney, M. S., Bombar, G. and Aksoy, A. O. 2013. Experimental study of the coarse surface development effect on the bimodal bed-load transport under unsteady flow conditions. *Journal of Hydraulic Engineering* 139: 12–21.

Göğüş, M. und Define, Z. 2005. Effect of Shape on Incipient Motion of Large Solitary Particles. *Journal of Hydraulic Engineering* 131: 38–45.

Hassan, M. A., R. Egozi, and G. Parker (2006), Experiments on the effect of hydrograph characteristics on vertical grain sorting in gravel bed rivers, *Water Resour. Res*., 42: W09408.

Jain, S. C. 1990. Armor or Pavement. *Journal of Hydraulic Engineering* 116(3): 436–440.

Kuhnle, R. A. 1993. Incipient motion of sand-gravel sediment mixtures. *Journal of Hydraulic Engineering*, 119(12): 1400–1415.

Mao, L., Cooper, J. R., and Frostick, L. E. 2011. Grain size and topographical differences between static and mobile armour layers. *Earth Surf. Process. Landforms* 36(10): 1321–1334.

Parker, G., Klingeman, P. C., and McLean, D. G. 1982. Bedload and size distribution in paved gravel-bed streams. *Journal of the Hydraulics Division* 108(4): 544–571.

Parker, G., and Sutherland, A. J. 1990. Fluvial armor. *Journal of Hydraulic Research* 28(5): 529–544.

Schendel, A., Goseberg, N., and Schlurmann, T. 2015. Erosion Stability of Wide-Graded Quarry-Stone Material under Unidirectional Current. *J. Waterway, Port, Coastal, Ocean Eng*., doi.org:10.1061/(ASCE)WW.1943-5460.0000321.

Shields, A. 1936. Anwendung der Ähnlichkeitsmechanik und der Turbulenzforschung auf die Geschiebebewegung. *Mitteilungen der Preußischen Versuchsanstalt für Wasserbau und Schiffbau*, Berlin (in German).

Shvidchenko, A. B., Pender, G., and Hoey, T. B. 2001. Critical shear stress for incipient motion of sand/gravel streambeds. *Water Resources Research* 37(8): 2273–2283.

Spiller, S. M., Rüther, N. and Baumann, B. 2015a. Form-induced stress in non-uniform steady and unsteady open channel flow over a static rough bed. *International Journal of Sediment Research* 30: 297–305.

Spiller, S. M., Rüther, N. and Friedrich, H. 2015b. Dynamic lift on an artificial armor layer during highly unsteady channel flow. *Water* 7: 4951–4970.

Wilcock, P. R. 1993. Critical shear stress of natural sediments. *Journal of Hydraulic Engineering* 119(4): 491–505.